Luminescence Enhancement of Pyrene/Dispersant Nanoarrays Driven by the Nanoscale Spatial Effect on Mixing

Kuan-Hsin Lo,[†] Ming-Chia Li,[†] Rong-Ming Ho,*,[†,⊥] Yuan-Chun Zhao,[§] Florian Massuyeau,[§] Wei-Tsung Chuang,[∥] Jean-Luc Duvail,*,[§] Serge Lefrant,[§] and Chain-Shu Hsu*,[‡]

[†]Department of Chemical Engineering, National Tsing Hua University, Hsinchu 30013, Taiwan

[‡] Department of Applied Chemistry, National Chiao Tung University, Hsinchu 30013, Taiwan

[§]Institut des Matériaux Jean Rouxel, UMR6502 CNRS, University of Nantes, F-44322 Nantes, France

[∥]National Synchrotron Radiation Research Center, Hsinchu 30076, Taiwan

[⊥]Frontier Research Center on Fundamental and Applied Sciences of Matters, Hsinchu 30013, Taiwan

Ⓢ *Supporting Information*

ABSTRACT: This work presents a simple method to generate ordered chromophore/dispersant nanoarrays through a pore-filling process for a nanoporous polymer template to enhance chromophore luminescence. Fluorescence results combining with the morphological evolution examined by scanning probe microscopy reveal that the enhanced luminescence intensity reaches the maximum intensity as the nanopores of the template are completely filled by the chromophore/dispersant mixture. The variation is attributed to nanoscale spatial effect on the enhanced mixing efficiency of chromophore and dispersant, that is, the alleviation of self-quenching problem, as evidenced by the results of attenuated total reflection Fourier transform IR spectroscopy combining with grazing incident wide-angle X-ray diffraction. The enhanced luminescence of the chromophore/dispersant nanoarrays driven by the nanoscale spatial effect is highly promising for use in designing luminescent nanodevices.
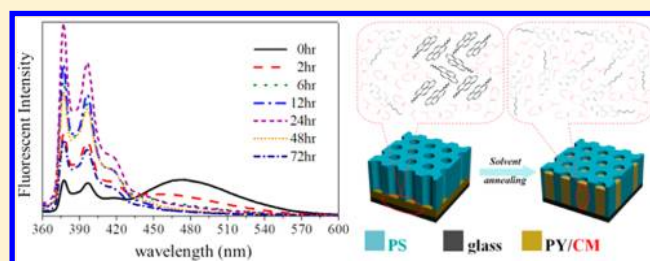
■ INTRODUCTION

As a well-known chromophoric material, pyrene is characterized by its long-lived excited state and the sensitivity of its excitation spectra to microenvironmental changes.[1] Notably, its luminescence can be adequately defined by controlling the intermolecular distance (z) between two pyrene molecules to form monomer ($z > 1$ nm) and excimer (0.4 nm $< z < 1$ nm).[1a,2] Owing to the high detected sensitivity of fluorescent properties,[1g] the pyrene molecule is frequently used as a fluorescent probe to monitor the phase transitions in polymers, either as a physical mixture[3] or a labeled polymer with the pyrene molecule chemically attached to the polymer chain.[4] Moreover, the pyrene molecule has received considerable attention due to its specific electrical and optical properties that are promising for the applications of nanotechnologies. For instance, by taking advantage of self-assembly, the intermolecular interaction has been exploited to form a well-ordered columnar stack from the pyrene molecules for investigating the charge transport in one-dimensional semiconducting organic nanostructures.[5] Also, strong hydrogen bonding and $\pi-\pi$ stacking between 1-pyrylphosphonic acid molecules have been used to generate a two-dimensional laminate architecture for the applications of field-effect transistors.[6] Those techniques are very useful to create self-assembled pyrene materials with desirable properties for device applications.[7]

However, precisely controlling nanostructure to give the specific properties of the pyrene molecule is challenging, particularly in a thin-film system. The self-assembly of soft matter is a highly convenient means of forming nanostructures with specific functions and complexity. The self-assembly of block copolymers (BCPs) that is driven by the incompatibility of constituent blocks can be exploited to fabricate nanomaterials with controlled geometries and unique functions. Accordingly, nanostructures from the self-assembly of BCPs, in particular, nanostructured thin films, are ideal templates for the formation of nanostructured hybrids and nanocomposites.[8] BCP thin-film samples with nanoporous textures can be obtained by chemically removing one constituent block using UV,[9] oxygen plasma,[10] ozone exposure,[11] and base aqueous solution.[12] Our previous studies have synthesized a series of polylactide-containing BCPs to construct a nanoporous polystyrene (PS) template from the self-assembly of the BCPs after hydrolysis of the polylactide blocks.[12b,13] A successful pore-filling process for the nanoporous PS template has been developed to create hybridized materials by exploiting the capillary force associated with tunable wetting property of

cadmium ions (Cd^{2+}) precursor solution. Consequently, CdS nanocrystals can be in situ generated by exposing the BCP template incorporated with cadmium acetate to H$_2$S vapor.[14] The nanoporous PS template has also been used as coatings on implantable devices for the control of drug delivery through pore-filling sirolimus, a potent immunosuppressive drug.[15] Also, a straightforward and effective method for fabricating patterned carbon nanotube (CNT) nanoarrays was developed by using the nanoporous PS template for Ni deposition via electroplating so as to serve as catalytic nanoarrays for the growth of CNTs.[16] Moreover, a new hybridization platform technology was developed using the nanoporous PS template for templated reactions so as to create hybridized materials with well-defined, oriented nanostructures.[17]

In this study, we aim to pore-fill a mixture of pyrene and dispersant into the nanoporous PS template so as to examine the nanoscale spatial effect on the fluorescence intensity of pyrene monomer emission in the nanostructured thin film. Through a specific pore-filling process, that is, a solvent-annealing process, the pyrene/dispersant mixture can be introduced into the template to form well-defined pyrene/dispersant nanoarrays (as shown in Figure 1). In contrast to a
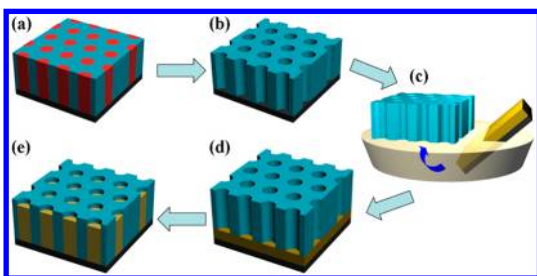

Figure 1. Schematic illustration of a nanoporous PS template pore-filled by a 1-pyrenebutanol/3-isochromanone (PY/CM) mixture through the solvent-annealing process. (a) Polystyrene-*b*-poly(L-lactide) (PS-PLLA) thin film; (b) nanoporous PS template from the PS-PLLA thin film after hydrolysis; (c) nanoporous PS template floated on water surface and collected by a PY/CM coated glass slide; (d) nanoporous PS template on a PY/CM thin film coated glass slide for the solvent-annealing process; (e) forming templated PY/CM nanoarrays after the solvent-annealing process.

simple pyrene/dispersant mixture, the fluorescence intensity of the pyrene monomer emission is significantly enhanced. This enhanced luminescence suggests that the forming nanostructured thin film significantly alleviates the self-quenching problem of the pyrene molecule. The changes in luminescence behavior are attributed to the enhanced mixing efficiency of the chromophore and dispersant.

■ EXPERIMENTAL SECTION

Synthesis of Polystyrene-*b*-poly(L-lactide) Block Copolymers. Polystyrene-*b*-poly(L-lactide) (PS-PLLA) diblock copolymers with a PLLA volume fraction of 0.25 were prepared by two-step living polymerization in sequence.[13]

Preparation of Nanoporous PS Template Pore-Filled by a 1-Pyrenebutanol/3-Isochromanone Mixture through the Solvent-Annealing Process. As illustrated in Figure 1, a thin-film sample with perpendicular cylindrical nanostructures is initially formed onto a glass substrate by spin coating (1000 rpm) from a 1.0 wt % chlorobenzene solution of PS-PLLA at 50 °C (Figure 1a); the film thickness is about 60 nm. After drying in a vacuum overnight, the film is exposed to UV radiation with the wavelength of 254 nm under a vacuum for over 10 min to enhance the adhesion of the thin film with

the substrate via hydrogen bonding between the hydroxyl group at the side chain of PS and the hydroxyl group at the surface of the glass substrate.[18] The thin-film sample is then placed in a NaOH solution for 4 days to degenerate PLLA (Figure 1b) and finally dispersed in a MeOH solution to wash out residual solution from degradation. After hydrolysis, the nanoporous PS templates were stained by exposing the samples to the vapor of a 4% aqueous RuO$_4$ solution for 30 s. The RuO$_4$ attacks the double bonds in the PS blocks, rendering the PS matrix cross-link and to promote the strength of the matrix. The nanoporous PS template is then used for pore-filling of a 1-pyrenebutanol/3-isochromanone (PY/CM) mixture; the 1-pyrenebutanol and 3-isochromanone were purchased from Aldrich. Subsequently, the template is removed from a glass substrate using 1% HF solution to dissolve the glass, floated onto an aqueous surface (Figure 1c), and finally, collected by a glass substrate coated with the PY/CM thin film (Figure 1d), resulting from spin coating (1000 rpm) from a 2 wt % ethanol solution of the PY/CM mixture. The film thickness of the PY/CM mixture is approximately 110 nm. The weight ratio of the PY/CM mixture is 1:15. The PY/CM is introduced into the pores driven by capillary force through solvent annealing using ethanol vapor at 70 °C (Figure 1e). The thin-film samples (forming templated PY/CM nanoarrays) at different solvent-annealing times were then examined by using UV−visible (UV−vis), fluorescence (FL), attenuated total reflection Fourier transform IR (ATR-FTIR) spectroscopic, and grazing incident wide-angle X-ray diffraction (GI-WAXD) experiments. The GI-WAXD measurement was performed with X-rays of a wavelength of 1.3336 Å on the diffractometer at the 17A diffraction beamline of the National Synchrotron Radiation Research Center (NSRRC), Taiwan. The control was commercially obtained AAO membranes with an average AAO pore diameter and thickness of 100−200 nm and 60 μm, respectively. Following the successful procedure for pore-filling agents by using the AAO membrane, several drops of 15 wt % PY/CM solution in ethanol were placed onto a glass substrate. Next, an AAO membrane was immediately placed on the top of the solution, and then, the nanopores of the membrane were filled with the PY/CM solution within seconds by a capillary force. Following solvent evaporation at ambient conditions, the pore-filled AAO membrane was dispersed in an ethanol solution to wash out residual PY/CM on the surface in order to form templated PY/CM microarrays.

■ RESULTS AND DISCUSSION

Figure 1 illustrates the fabrication process of nanoporous PS template pore-filled by a PY/CM mixture through the solvent-annealing process. Owing to the degradable character of the polyester component,[12a] the hydrolysis of PS-PLLA provides a simple method of preparing a nanoporous PS. A thin-film template with large-scale, oriented cylindrical nanochannels can be obtained from the self-assembly of PS-PLLA for nanostructuring thin films followed by hydrolysis.[12b] Figure 2 displays the transmission electron microscopy (TEM) images of the nanoporous PS and templated PY/CM nanoarrays. As shown in Figure 2a, hexagonally packed cylindrical nanopores can be obtained by hydrolyzing the PS-PLLA thin film at which the nanoporous PS appears as gray matrix and the nanopores (approximately 20 nm in diameter) are bright regions because of the mass−thickness contrast resulting from RuO$_4$ staining. After the solvent-annealing process for pore-filling the PY/CM mixture into the cylindrical nanochannels of the nanoporous PS, the PY/CM mixture can be successfully introduced into the nanopores of the PS template. Consequently, templated PY/CM nanoarrays can be formed as evidenced by the TEM micrograph of Figure 2b at which inversed mass−thickness contrast with a significant dark contrast dispersed in the light gray PS matrix can be clearly identified due to the enhancement of the mass−thickness contrast of the PY/CM mixture by using potassium phosphotungstate (PTA) for staining.
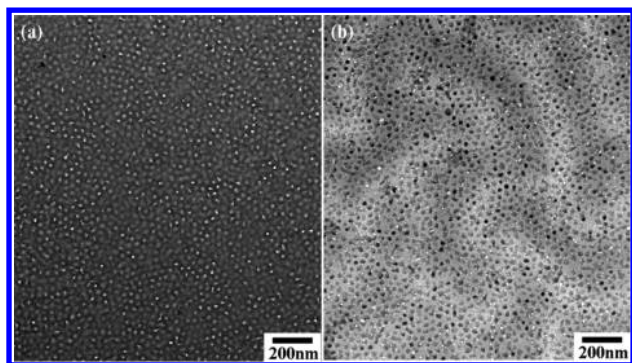
Figure 2. TEM images of (a) cylindrical nanoporous PS template from a hydrolytic PS-PLLA thin film using RuO$_4$ for staining; (b) templated PY/CM nanoarrays using PTA for staining.

Steady-state FL spectra were acquired to determine the luminescent behavior of a spin-coated PY/CM thin film and templated PY/CM nanoarrays. As shown in Figure 3a, the monomer emission band consisting of three emission peaks at 378, 392, and 421 nm and a broad emission band centered at 476 nm attributed to the formation of excimer (i.e., pyrene molecules associated in the ground state) appear for the spin-coated PY/CM thin film.[1g] After solvent annealing (i.e., the introduction of the PY/CM matrix into the nanopores), the FL intensity of monomer emission significantly increases whereas the intensity of excimer emission slightly decreases. To quantitatively examine the variations on the relative intensities between the excimer and monomer bands, the excimer/monomer emission ratio (I_E/I_M) was calculated by comparing the fluorescence intensity of the excimer band at 476 nm to that of the first monomer peak at 378 nm. As shown in Figure 3a, the excimer/monomer emission ratio (I_E/I_M) significantly decreases from 0.94 to 0.13 after solvent annealing, indicating an increase of intermolecular distance between pyrene molecules within the nanochannels via solvent annealing. For comparison, the spin-coated PY/CM thin film without using the PS template was treated by the same solvent-annealing process. As shown in Figure 3b, the intensities of monomer and excimer emissions for the PY/CM mixture both significantly decrease after solvent annealing. The enhanced luminescence for the templated PY/CM nanoarrays resembles the behavior of the pyrene molecules in nucleotide−monophosphates micellar solution in which small molecules can be used to induce an increment in the FL intensity of pyrene due to the increase on the dispersion of the pyrene molecule in the micelle so as to

alleviate the self-quenching problem.[19] Consistently, similar results of the disappearance of excimer emission and the increase in the intensity of monomer emission due to the mixing of pyrene in the PS core of the nanoparticle in the solution state can be found.[20] As a result, we speculate that the inhibition of the self-quenching phenomenon resulting in the enhanced luminescence nanostructured PY/CM thin film is attributed to the improvement in the dispersion of the PY in the PY/CM mixture due to the nanoscale spatial effect.

To further examine the suggested nanoscale spatial effect on the luminescent behavior for the comparison with the results from the templated PY/CM nanoarrays, submicroscale AAO membrane was used as a template for the pore-filling PY/CM mixture to prepare templated PY/CM submicroarrays. The AAO membrane is a commercial product with an AAO pore diameter ranging from 100 to 200 nm and a thickness of 60 μm on average. After removal of the AAO template, templated PY/CM submicroarrays can be obtained (Figure 4a). The diameter of the PY/CM cylinder is approximately equal to the pore size of the AAO membrane, indicating the successful process for templating. However, as shown in Figure 4b, no significant change with respect to the FL intensities of monomer and excimer emissions before and after solvent annealing can be found. As reported by Hillmyer and co-workers, hydroxyl groups on the internal surface of nanopores could be obtained after hydrolysis of polystyrene-b-poly(D, L-lactide) (PS-PLA).[21] As a result, it is reasonable to suggest that the surface property of the inner wall for the nanopore resulting from hydrolysis of PS-PLLA is similar to that for the submicropore of the AAO membrane. Also, as examined in this study, the FL results in Figure 4b indicate that the effect of the aspect ratio of the channel length to diameter is not critical to the enhanced luminescence. Furthermore, the intensities of monomer emission of the PY/CM mixture within the nanoporous PS template (Figure 3a) are much higher than the ones in the AAO membrane (Figure 4b) via solvent annealing. Consequently, the discrepancies on the luminescent behavior between the pore-filling PY/CM mixture within the nanoporous PS template and the AAO membrane should be truly attributed to the variation of pore size. In other words, the nanoscale spatial effect on the luminescence behavior of the pore-filling PY/CM mixture within the PS template did play an important role to significantly increase the intensity of monomer emission.

To further identify the suggested nanoscale spatial effect on the luminescent behavior, the FL spectra of templated PY/CM nanoarrays through solvent annealing at various annealing
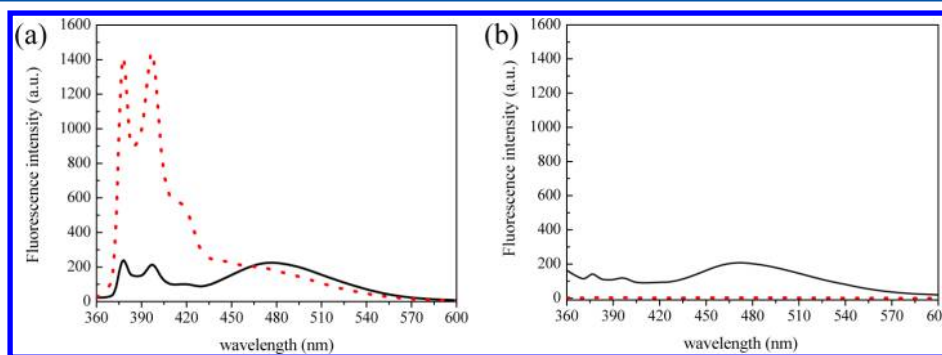

Figure 3. FL spectra of spin-coated PY/CM thin films on glass substrates (a) with; (b) without the deposition of nanoporous PS template before (solid line) and after (dotted line) solvent annealing.
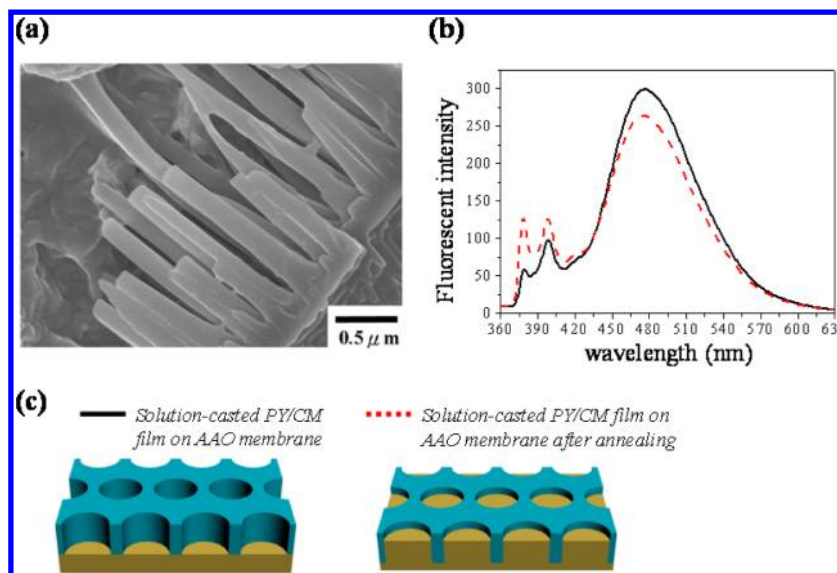
Figure 4. (a) Field emission scanning electron microscopy image of the templated PY/CM submicroarrays after removal of the AAO membrane; (b) FL spectra of the solution-cast polymer film on a glass substrate with the deposition of the AAO membrane before (solid line) and after (dashed line) ethanol solvent annealing; (c) schematic illustration of the solution-cast polymer film on a glass substrate with the deposition of the AAO membrane before and after ethanol solvent annealing.

times were acquired. The corresponding morphological evolution was traced by using scanning probe microscopy (SPM). Figure 5a shows the FL spectra of the templated PY/
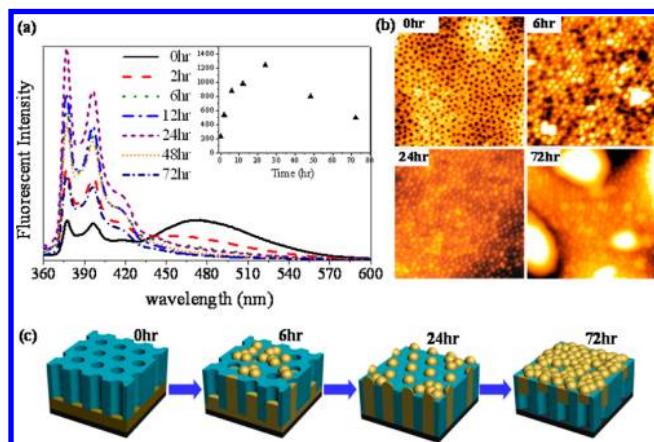

Figure 5. (a) FL spectra of templated PY/CM nanoarrays through solvent-annealing at different annealing times. Inset shows the plot of the intensity of monomer emission (378 nm) versus annealing time. (b) SPM tapping-mode height images of the nanoporous PS template on the spin-coated PY/CM thin film at different solvent-annealing times. The scale of the SPM image is 1 μm × 1 μm. (c) Schematic illustration of the morphological evolution of pore-filling PY/CM.

CM nanoarray through solvent-annealing at different annealing times. The FL intensity of monomer emission increases with annealing time whereas the intensity of excimer emission decreases with annealing time. Also, all of the monomer emission peaks show a blueshift with annealing time. These FL results suggest that the solvent-annealing process would give rise to the separation of PY molecules in the templated PY/CM nanoarray due to the improved dispersion of the PY in the PY/CM mixture. Furthermore, as shown in the inset of Figure 5a, the FL intensity of monomer emission increases and then reaches the maximum intensity at 24 h whereas the excimer

emission decreases with annealing time. Upon further annealing, the intensity of monomer emission decreases significantly. Figure 5b shows the corresponding morphological evolution of thin-film topography in which the initial morphology reveals the topographic surface of the nanoporous PS template. Notably, to ensure that the nanoporous PS template can be completely filled with the PY/CM mixture, a thick enough PY/CM thin film was used for pore-filling. Also, the FL experiments were carried out by using the whole set of templated system so as to provide a systematic comparison with respect to the variation on the FL intensity during solvent annealing. With increasing annealing time, the increase in the area of protrusion (i.e., the surfaced PY/CM mixture) due to the overflow of pore-filled mixture can be clearly recognized. At 24 h, the protrusion can be found in most of the nanopores. Generally, the driving force of pore-filling results from a capillary force that is dependent upon the surface tension of the wetting substrate (i.e., PS template) and the wetting tendency for the solution onto the substrate (i.e., the interfacial energy of PS and solution).[16,17a] Ethanol vapor is used to promote the wetting tendency of the PY/CM mixture for pore-filling through capillary rise. The capillary rise of a polymeric liquid in a nanoporous template has been studied recently; note that the occurrence of an overflow of polymer melt onto the surface is usually expected.[22] Similarly, the PY/CM mixture tends to surface out from the nanopore due to the affinity of ethanol vapor with the mixture; after 72 h of solvent annealing, the formation of islandlike texture on the top of the PS template can be found because of the merging of surfaced PY/CM mixture. The morphological evolution corresponds well with the observed changes on the FL spectra of the pore-filled PY/CM mixture. Once the PY/CM mixture releases from the nanopores through pore-filling, the nanoscale spatial effect on the PY/CM mixture releasing from the nanopores is annihilated so as to cause a significant self-quenching problem again. Also, after the mixture releasing from the nanopores, the intensity of excimer emission is different to the intrinsic one. We speculate that the variation is attributed to the solvent
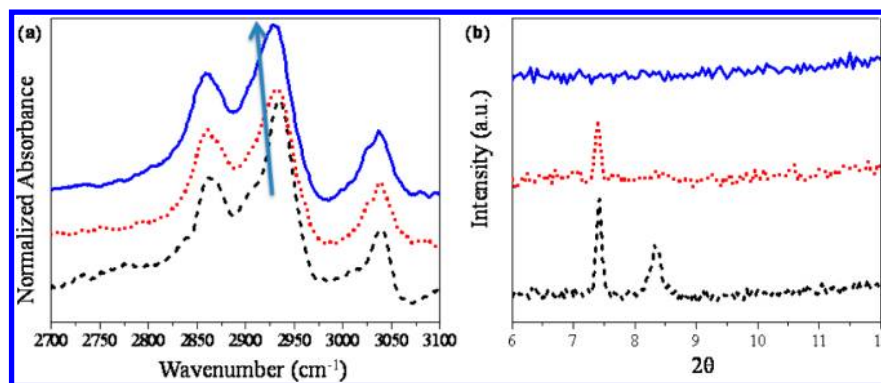
Figure 6. (a) ATR-FTIR spectra and (b) GI-WAXD profiles of the spin-coated PY thin film (dashed line), the nanoporous PS template on the PY/CM thin film (dotted line), and the templated PY/CM nanoarrays (solid line).

annealing effect on the phase behavior of the mixture. Similar phenomena can also be found in the solvent-annealed PY/CM thin film without using the template; as shown in Figure 3b, solvent annealing would cause a significant self-quenching problem and also lower the intensity of excimer emission. As a result, there is no issue of the reappearance of significant excimer emission after solvent annealing.

To further examine the origins of the nanoscale spatial effect on the luminescent behavior, UV−vis and ATR-FTIR spectroscopic experiments were carried out on the templated PY/CM nanoarrays. Figure S1 of Supporting Information shows the absorption spectra of PY and the PY/CM mixture with intense bands in the range 260−380 nm, which is referred to as the PY absorption.[1g] In contrast to the absorption of the neat PY thin film, the absorption spectrum of the solvent-annealed PY/CM nanoarray show a blueshift of approximately 9 nm whereas the absorption of the PY/CM thin film before solvent-annealing shows a blueshift of approximately 8 nm. These results reflect that the dispersion of PY in the PY/CM mixture is significantly increased.[23] As a result, we suggest that the variation on the luminescent behavior of the templated PY/CM nanoarrays is attributed to the improved dispersion of PY in the PY/CM mixture (i.e., the enhanced mixing efficiency of PY and CM) resulting from the nanoscale spatial effect. ATR-FTIR results further demonstrate the improvement in dispersion due to the nanoscale spatial effect. As shown in Figure 6a, the absorption peak at 3038 cm^{-1} is referred to as the C−H stretching vibration with a sp^2 CH hybridized carbon atom corresponding to the phenyl in the PY molecule. The peaks at 2862 and 2935 cm^{-1} are attributed to the sp^3 CH symmetric and antisymmetric stretching vibrations,[24] respectively, corresponding to the alkyl chain of the PY tail. For the PY/CM mixture, the absorption peaks of the CH stretching corresponding to the alkyl chain of PY tail experience a redshift while the peak at 3038 cm^{-1} remains unchanged. It is reasonable to suggest that the changes of the frequencies of sp^3 CH stretching vibrations are attributed to the improved dispersion of PY in the PY/CM mixture. Moreover, a noticeable discrepancy between the redshifts in the intrinsic PY/CM mixture and the templated PY/CM nanoarrays (3 and 6 cm^{-1}, respectively) can be identified. The redshifts are attributed to the relaxation of the C−H bond distance in the alky chain of the PY tail.[25] Notably, the excimer emission of the pyrene molecule results from the geometry of the dimer, and the formation of the dimer is attributed to π−π interaction.[1g] The structure of the dimer consists of partially overlapping card-packed dimeric units with pyrene parallel texture, and the

crystalline structure is the result of the packing of the dimeric units.[26] Accordingly, the excimer emission is usually dependent upon the crystallinity of the pyrene molecule whereas the self-quenching behavior is attributed to the preassociation of pyrene molecules inside nonemission pyrene aggregation.[27] As a result, the self-quenching behavior resulting from aggregation does not correspond with the formation of excimer.

The suggested nanoscale spatial effect leads to the increase in the dispersion of PY in the PY/CM mixture so as to reduce the formation of self-quenching aggregates. As reported by Winnik and co-workers, significant increase in the monomer emission of pyrene primarily results from the alleviation of the self-quenching problem corresponding to nonemissive aggregates in aqueous pyrene-labeled polymer solutions.[28] Consequently, we suggest that the conformational change of PY is attributed to the releasing of the alkyl chain from the ordered aggregates of PY molecules so as to result in the redshift in the ATR-FTIR absorption. To further examine the variation of luminescent behavior driven by the nanoscale spatial effect, GI-WAXD experiments using a synchrotron radiation source was performed to examine the morphological variation of self-assembled PY aggregates in the PY/CM mixture as thin films. Consistent to the WAXD results of bulk samples (see Figure S2 of the Supporting Information), one characteristic peak of the crystalline structure of PY was identified at the 2θ value of 7.43° for the spin-coated PY thin film (see the dashed line of Figure 6b). Note that the chromophore examined here is PY (that is pyrene with a functional tail) but not pyrene so that the crystalline structure should be slightly different to that of pyrene. By contrast, for the PY/CM mixture, this characteristic peak shifts to 7.40° (see the dotted line of Figure 6b). The distances calculated by $2d \sin \theta = n\lambda$ ($\lambda = 1.33$ Å) for 2θ = 7.43° and 7.40° are 10.26 and 10.30 Å, respectively, suggesting that the spacing variation (approximately 0.04 Å increase on the crystalline spacing) is attributed to the dispersion effect resulting from the introduction of dispersant (that is CM). This characteristic scattering peak disappears for the templated PY/CM nanoarrays (Figure 6b). Namely, the formation of templated PY/CM nanoarrays gives rise to the changes of the morphology of PY aggregates at which the card-packed structure from the ordered agates can be released by pore-filling the PY/CM mixture into the PS template. Moreover, on the basis of the PL results at which a significant decrease in the excimer emission can be found, it is reasonable to suggest that the nanoscale spatial effect on the dispersion of PY in the PY/CM mixture also disassociates the overlapping card-packed dimeric units. Accordingly, significant enhancement on

luminescence can be acquired by pore-filling the PY/CM mixture into the nanopores due to the nanoscale spatial effect, leading to the disassociation of the PY crystalline form and card-packed dimeric units by separating the PY molecules with the CM molecules so as to alleviate the self-quenching problem. Consequently, the compressed alkyl tails of the PY molecules might be liberated from the crystalline structure, subsequently increasing the dispersion of PY in the PY/CM mixture with freely stretched tails after the pore-filling process, as illustrated in Figure 7.
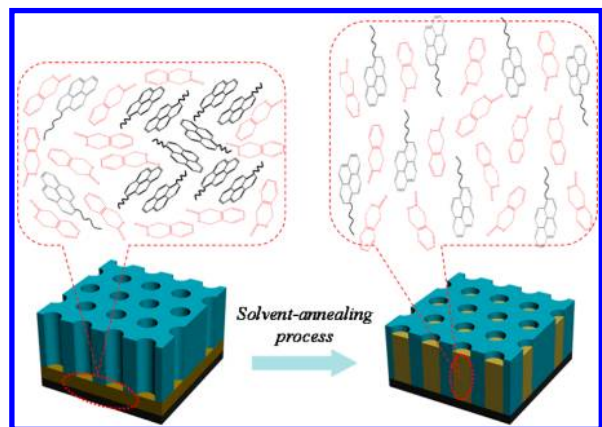

Figure 7. Schematic illustration of molecular dispositions for the spin-coated PY/CM thin film before solvent annealing and templated PY/CM nanoarrays.

CONCLUSIONS

In summary, this work developed a simple method to generate ordered PY/CM nanoarrays through a pore-filling process, subsequently enhancing the PY luminescence. The enhanced luminescence is attributed to the improved dispersion of PY in the PY/CM mixture driven by the nanoscale spatial effect for a pore-filled mixture. As evidenced by the SPM and FL results, the variation on the intensity of PY emission is in line with the progress of a specific pore-filling process. Owing to the enhanced mixing efficiency of PY and CM, the self-quenching problem of the PY luminescence resulting from nonemission PY aggregation can be significantly alleviated. This work also characterized the molecular dispositions of the PY/CM mixture by ATR-FTIR and GI-WXAD experiments, demonstrating the nanoscale spatial effect on the enhancement of the mixing efficiency of PY and CM. As a result, the formation of templated PY/CM nanoarrays gives rise to the changes of the morphology of PY aggregates at which the card-packed structure from the ordered agates can be released by pore-filling the PY/CM mixture into the nanopores of the PS template. Consequently, the enhanced luminescence of the PY/CM mixture driven by the nanoscale spatial effect is highly promising for use in designing luminescent nanodevices.

ASSOCIATED CONTENT

Ⓢ Supporting Information
Additional details on the preparation of templated PY/CM microarrays, UV–vis spectra, and wide-angle X-ray diffraction patterns. This material is available free of charge via the Internet at http://pubs.acs.org.

AUTHOR INFORMATION

Corresponding Author
*E-mail: rmho@mx.nthu.edu.tw (R.-M.H.).

Notes
The authors declare no competing financial interest.

ACKNOWLEDGMENTS

REFERENCES

(1) (a) Birks, J. B. Excimers. *Rep. Prog. Phys.* **1975**, *38*, 903. (b) Birks, J. B.; Christophorou, L. G. Excimer fluorescence spectra of pyrene derivatives. *Spectrochim. Acta* **1963**, *19*, 401. (c) Birks, J. B.; Dyson, D. J.; Munro, I. H. 'Excimer' fluorescence. II. Lifetime studies of pyrene solutions. *Proc. R. Soc. London, Ser. A* **1963**, *275*, 575. (d) Avis, P.; Porter, G. Effect of concentration on the absorption and fluorescence spectra of pyrene in a solid solution of poly(methyl methacrylate). *J. Chem. Soc., Faraday Trans. 2* **1974**, *70*, 1057. (e) Johnson, G. E. Effect of concentration on the fluorescence spectra and lifetimes of pyrene in polystyrene films. *Macromolecules* **1980**, *13*, 839. (f) Yanagimachi, M.; Toriumi, M.; Masuhara, H. Selective incorporation and aggregation of pyrene in a segmented poly(urethane urea) film as revealed by picosecond total internal reflection fluorescence spectroscopy. *Chem. Mater.* **1991**, *3*, 413. (g) Winnik, F. M. Photophysics of preassociated pyrenes in aqueous polymer solutions and in other organized media. *Chem. Rev.* **1993**, *93*, 587. (h) Wilhelm, M.; Zhao, C. L.; Wang, Y. C.; Xu, R. L.; Winnik, M. A.; Mura, J. L.; Riess, G.; Croucher, M. D. Poly(styrene-ethylene oxide) block copolymer micelle formation in water: a fluorescence probe study. *Macromolecules* **1991**, *24*, 1033. (i) Jhaveri, S. B.; Beinhoff, M.; Hawker, C. J.; Carter, K. R.; Sogah, D. Y. Chain-end functionalized nanopatterned polymer brushes grown via in situ nitroxide free radical exchange. *ACS Nano* **2008**, *2*, 719. (j) Battistini, G.; Cozzi, P. G.; Jalkanen, J. P.; Montalti, M.; Prodi, L.; Zaccheroni, N.; Zerbetto, F. The erratic emission of pyrene on gold nanoparticles. *ACS Nano* **2008**, *2*, 77. (k) Sagara, Y.; Kato, T. Stimuli-responsive luminescent liquid crystals: change of photoluminescent colors triggered by a shear-induced phase transition. *Angew. Chem., Int. Ed.* **2008**, *47*, 5175.

(2) Winnik, M. A. End-to-end cyclization of polymer chains. *Acc. Chem. Res.* **1985**, *18*, 73.

(3) (a) Ellison, C. J.; Torkelson, J. M. Sensing the glass transition in thin and ultrathin polymer films via fluorescence probes and labels. *J. Polym. Sci., Part B: Polym. Phys.* **2002**, *40*, 2745. (b) Martins, T. D.; Yamaki, S. B.; Prado, E. A.; Atvars, T. D. Z. Broadening of the fluorescence spectra of hydrocarbons in ethylene-vinyl acetate copolymers and the dynamics of the glass transition. *J. Photochem. Photobiol., A* **2003**, *156*, 91.

(4) (a) Winnik, M. A.; Redpath, A. E. C.; Richards, D. H. The dynamics of end-to-end cyclization in polystyrene probed by pyrene excimer formation. *Macromolecules* **1980**, *13*, 328. (b) Winnik, M. A.; Redpath, A. E. C.; Paton, K.; Danhelka, J. Cyclization dynamics of polymers: 10 Synthesis, fractionation, and fluorescent spectroscopy of pyrene end-capped polystyrenes. *Polymer* **1984**, *25*, 91.

(5) Nguyen, T. Q.; Martel, R.; Avouris, P.; Bushey, M. L.; Brus, L.; Nuckolls, C. Molecular interactions in one-dimensional organic nanostructures. *J. Am. Chem. Soc.* **2004**, *126*, 5234.

(6) Yip, H. L.; Ma, H.; Jen, A. K.-Y.; Dong, J.; Parviz, B. A. Two-dimensional self-assembly of 1-pyrylphosphonic acid: transfer of stacks on structured surface. *J. Am. Chem. Soc.* **2006**, *128*, 5672.

(7) Li, M. C.; Ho, R. M.; Lee, Y. D. Photo-induced excimer formation of pyrene-labeled polymers for optical recording. *J. Mater. Chem.* **2011**, *21*, 2451.

(8) (a) Bates, F. S.; Fredrickson, G. H. Block copolymer thermodynamics: theory and experiment. *Annu. Rev. Phys. Chem.* **1990**, *41*, 525. (b) Morkved, T. L.; Lu, M.; Urbas, A. M.; Ehrichs, E.

E.; Jaeger, H. M.; Mansky, P.; Russell, T. P. Local control of microdomain orientation in diblock copolymer thin films with electric fields. *Science* **1996**, *273*, 931. (c) Mansky, P.; Liu, Y.; Huang, E.; Russell, T. P.; Hawker, C. Controlling polymer-surface interactions with random copolymer brushes. *Science* **1997**, *275*, 1458. (d) Cheng, J. Y.; Ross, C. A.; Chan, V. Z.-H.; Thomas, E. L.; Lammertink, R. G. H.; Vancso, G. J. Formation of a cobalt magnetic dot array via block copolymer lithography. *Adv. Mater.* **2001**, *13*, 1174. (e) Temple, K.; Kulbaba, K.; Power-Billard, K. N.; Manners, I.; Leach, K. A.; Xu, T.; Russell, T. P.; Hawker, C. J. Spontaneous vertical ordering and pyrolytic formation of nanoscopic ceramic patterns from poly(styrene-*b*-ferrocenylsilane). *Adv. Mater.* **2003**, *15*, 297. (f) Kim, S. H.; Misner, M. J.; Xu, T.; Kimura, M.; Russell, T. P. Highly oriented and ordered arrays from block copolymers via solvent evaporation. *Adv. Mater.* **2004**, *16*, 226.

(9) (a) Thurn-Albrecht, T.; Steiner, R.; DeRouchey, J.; Stafford, C. M.; Huang, E.; Bal, M.; Tuominen, M.; Hawker, C. J.; Russell, T. P. Nanoscopic templates from oriented block copolymer films. *Adv. Mater.* **2000**, *12*, 787. (b) Misner, M. J.; Skaff, H.; Emrick, T.; Russell, T. P. Directed deposition of nanoparticles using diblock copolymer templates. *Adv. Mater.* **2003**, *15*, 221. (c) Park, S.; Kim, B.; Wang, J. Y.; Russell, T. P. Fabrication of highly ordered silicon oxide dots and stripes from block copolymer thin films. *Adv. Mater.* **2008**, *20*, 681.

(10) Cheng, J. Y.; Ross, C. A.; Thomas, E. L.; Smith, H. I.; Vancso, G. J. Fabrication of nanostructures with long-range order using block copolymer lithography. *Appl. Phys. Lett.* **2002**, *81*, 3657.

(11) Park, M.; Harrison, C.; Chaikin, P. M.; Register, R. A.; Adamson, D. H. Block copolymer lithography: periodic arrays of ~10^{11} holes in 1 square centimeter. *Science* **1997**, *276*, 1401.

(12) (a) Zalusky, A. S.; Olayo-Valles, R.; Taylor, C. J.; Hillmyer, M. A. Mesoporous polystyrene monoliths. *J. Am. Chem. Soc.* **2001**, *123*, 1519. (b) Ho, R. M.; Tseng, W. H.; Fan, H. W.; Chiang, Y. W.; Lin, C. C.; Ko, B. T.; Huang, B. H. Solvent-induced microdomain orientation in polystyrene-*b*-poly(L-lactide) diblock copolymer thin films for nanopatterning. *Polymer* **2005**, *46*, 9362.

(13) (a) Ho, R. M.; Chiang, Y. W.; Lin, S. C.; Chen, C. K. Helical architectures from self-assembly of chiral polymers and block copolymers. *Prog. Polym. Sci.* **2011**, *36*, 376. (b) Ho, R. M.; Chiang, Y. W.; Tsai, C. C.; Lin, C. C.; Ko, B. T.; Huang, B. H. Three-dimensionally packed nanohelical phase in chiral block copolymers. *J. Am. Chem. Soc.* **2004**, *126*, 2704.

(14) Lo, K. H.; Tseng, W. H.; Ho, R. M. In-situ formation of CdS nanoarrays by pore-filling nanoporous templates from degradable block copolymers. *Macromolecules* **2007**, *40*, 2621.

(15) Lo, K. H.; Chen, M. C.; Ho, R. M.; Sung, H. W. Pore-filling nanoporous templates from degradable block copolymers for nano-scale drug delivery. *ACS Nano* **2009**, *3*, 2660.

(16) Tseng, Y. T.; Tseng, W. H.; Lin, C. H.; Ho, R. M. Fabrication of double-length-scale patterns via lithography, block copolymer templating, and electrodeposition. *Adv. Mater.* **2007**, *19*, 3584.

(17) (a) Tseng, W. H.; Chen, C. K.; Chiang, Y. W.; Ho, R. M.; Akasaka, S.; Hasegawa, H. Helical nanocomposites from chiral block copolymer templates. *J. Am. Chem. Soc.* **2009**, *131*, 1356. (b) Hsueh, H. Y.; Chen, H. Y.; Chen, C. K.; Ho, R. M.; Gwo, S.; Akasaka, S.; Hasegawa, H. Inorganic gyroid with exceptionally low refractive index from block copolymer templating. *Nano Lett.* **2010**, *10*, 4994. (c) Hsueh, H. Y.; Huang, Y. C.; Ho, R. M.; Lai, C. H.; Makida, T.; Hasegawa, H. Nanoporous gyroid nickel from block copolymer templates via electroless plating. *Adv. Mater.* **2010**, *23*, 3041.

(18) Yan, M.; Harnish, B. A simple method for the attachment of polymer films on solid substrates. *Adv. Mater.* **2003**, *15*, 244.

(19) Cuomoa, F.; Palazzob, G.; Cegliea, A.; Lopeza, F. Quenching efficiency of pyrene fluorescence by nucleotide monophosphates in cationic micelles. *J. Photochem. Photobiol., A* **2009**, *202*, 21.

(20) Kumar, V.; Adamson, D. H.; Prud'homme, R. K. Fluorescent polymeric nanoparticles: aggregation and phase behavior of pyrene and amphotericin B molecules in nanoparticle cores. *Small* **2010**, *24*, 2907.

(21) Zalusky, A. S.; Olayo-Valles, R.; Wolf, J. H.; Hillmyer, M. A. Ordered nanoporous polymers from polystyrene−polylactide block copolymers. *J. Am. Chem. Soc.* **2002**, *124*, 12761.

(22) Shin, K.; Obukhov, S.; Chen, J. T.; Huh, J.; Hwang, Y.; Mok, S.; Dobriyal, P.; Thiyagarajan, P.; Russell, T. P. Enhanced mobility of confined polymers. *Nat. Mater.* **2007**, *6*, 961.

(23) (a) Kunjappu, J. T.; Somasundaran, P. Aggregation behavior of 12-(1-pyrenyl)dodecanoic acid in homogeneous and micellar solutions. *Langmuir* **1995**, *11*, 428. (b) Dutta, A. K.; Misra, T. N.; Pal, A. J. A spectroscopic study of nonamphiphilic pyrene assembled in Langmuir−Blodgett films: formation of aggregates. *Langmuir* **1996**, *12*, 459.

(24) (a) Dischler, B.; Bubenzer, A.; Koidl, P. Bonding in hydrogenated hard carbon studied by optical spectroscopy. *Solid State Commun.* **1983**, *48*, 105. (b) Dischler, B.; Bubenzer, A.; Koidl, P. Hard carbon coating with low optical absorption. *Appl. Phys. Lett.* **1983**, *42*, 636.

(25) (a) Hobza, P.; Spirko, V.; Selzle, H. L.; Schlag, E. W. Anti-hydrogen bond in the benzene dimer and other carbon proton donor complexes. *J. Phys. Chem. A* **1998**, *102*, 2501. (b) Reimann, B.; Buchhold, K.; Vaupel, S.; Brutschy, B.; Havlas, Z.; Spirko, V.; Hobza, P. Improper, blue-shifting hydrogen bond between fluorobenzene and fluoroform. *J. Phys. Chem. A* **2001**, *105*, 5560.

(26) (a) Robertson, J. M.; White, J. G. 72. The crystal structure of pyrene. A quantitative X-Ray investigation. *J. Chem. Soc.* **1947**, 358. (b) Camerman, A.; Trotter, J. The crystal and molecular structure of pyrene. *Acta Crystallogr.* **1965**, *18*, 636.

(27) Anghel, D. F.; Alderson, V.; Winnik, F. M.; Misuzaki, M.; Morishima, Y. Fluorescent dyes as model 'hydrophobic modifiers' of polyelectrolytes: a study of poly(acrylic acid)s labeled with pyrenyl and naphthyl groups. *Polymer* **1998**, *39*, 3035.

(28) Winnik, F. M.; Regismond, S. T. A.; Goddard, E. D. Interactions of an anionic surfactant with a fluorescent-dye-labeled hydrophobically-modified cationic cellulose ether. *Langmuir* **1997**, *13*, 111.